A New Approach to Measuring the Sensitive Volume Using a Pulsed Laser System

R Jones, A M Chugg, P Jones
Radiation Effects Group, Matra BAe Dynamics, Filton, Bristol, England

R Harboe-Sorensen
ESA/ESTEC, Noordwijk, The Netherlands

R Fitzgerald, R Allison, T O'Shea
DTE Group, NMRC, Cork, Ireland

Abstract

Recent work has shown that ions can be used to measure the depth and thickness of the sensitive volume in memory devices and that laser pulsing at a range of wavelengths also yields an estimate of the charge collection depth. In this paper it is shown that the laser technique can be extended to provide a detailed measurement of the sensitivity profile of a memory cell with respect to charge collection from an ionisation track. It is also shown, through analysis of pulsed laser SEU threshold measurements made at two wavelengths, that the charge collection depth for 1Mbit SRAM's appears to be significantly greater than the depth of the active region.

I. INTRODUCTION

Laser testing (using large arrays of pulses) can imitate ion beam testing in deriving an LET threshold for upset or latchup [1]. However, the calculation of proton and neutron single event effects further requires a knowledge of the dimensions of the sensitive volume, since the basis of the extrapolation is that proton/neutron effects will be approximately the same as ion effects for the same energy depositions in the sensitive volume. Various approaches have been proposed for combining the sensitive volume information with the LET cross-section curve and proton/neutron interaction physics to derive the proton/neutron upset rate, e.g. [2], [3].

A reasonable estimate of the cross-section of the sensitive volume can be made from the saturation cross-section in ion beam or laser testing provided allowance is made for multiple bit upsets and metallisation shadowing. This leaves a requirement for a measurement of the effective thickness of the sensitive volume. Simulation work on this problem has recently been conducted by PJ McNulty et al [4]. An empirical method of using a beam of carbon ions at a range of energies in order to probe the depth and thickness of the sensitive region has recently been developed and tested by Inguimbert et al [5]. The Bragg peak in the ion's energy deposition profile is moved through the sensitive volume by increasing the ion's initial energy. In outline, the location of the sensitive region is inferred from the Bragg peak depth at which the upset rate peaks and its width can be derived from the range of Bragg peak depths over which upsets are observed. Furthermore, JS Melinger et al [6] have shown that laser pulse testing of electronic devices can yield an estimate of the charge collection depth.

The purpose of the present paper is to show that laser probing of the charge collection region at a suitable range of wavelengths can potentially yield the exact sensitivity profile of a memory cell with respect to charge collection from an ionisation track. (It should particularly be noted that this laser probing of the sensitivity profile is completely independent of any calibration against ion beam tests or other radiation source measurements.) In addition, actual laser SEU threshold measurements made on 1Mbit SRAM's at two wavelengths are shown to provide two types of indication that the charge collection depth for 1Mbit SRAM's is significantly greater than the depth of the active region. This implies that significant charge is being gathered from the substrate, perhaps via the funnel effect.

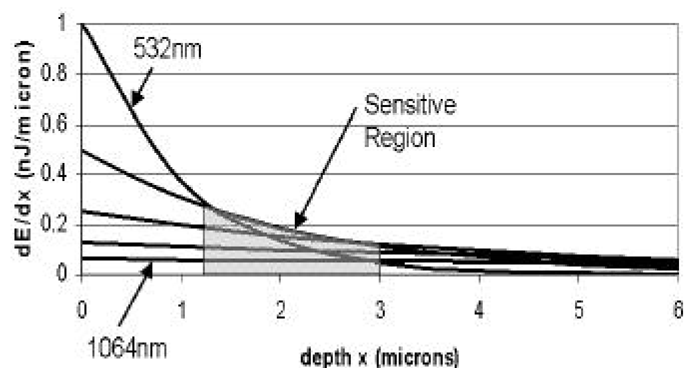

Figure 1: dE/dx for laser pulses of fixed energy at a range of wavelengths (green to infra red).

II. THEORY

The energy deposition profile for laser pulses in silicon is a decaying exponential, where the decay constant, which is known as the absorptivity, has an inverse relationship with the wavelength. At first sight it is not obvious how this type of profile can reproduce the Bragg peak effect to probe the sensitive region depth and thickness. However, on plotting the energy deposition profiles for a range of wavelengths at constant pulse energy, it can be seen (Figure 1) that the energy deposition in an arbitrary range of depth (1.3 to 3 microns for the present example) is a maximum at a wavelength in the middle of the range. It transpires that the peak energy

deposition wavelength is generally very sensitive to the depth and thickness of the sensitive region.

For this model, at a fixed pulse energy, there will in general exist upper and lower bounds on the range of laser wavelengths which give rise to upsets (Figure 2). In practice, the most straightforward experimental procedure is to vary the energy at a fixed wavelength to establish the upset threshold energy for that wavelength.

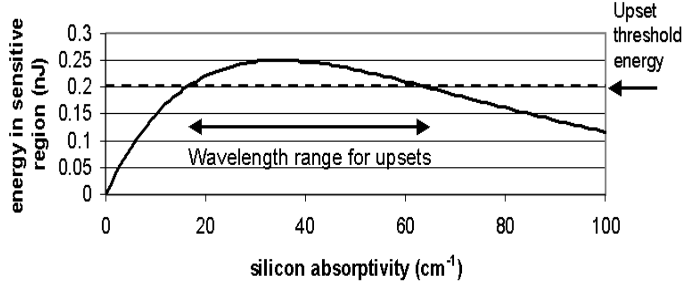

Figure 2: Variation of energy deposited in the sensitive layer with silicon absorptivity for laser pulses at a fixed energy (conceptual - NB wavelength decreases with increasing absorptivity).

For pulse energy E_p and reflected energy E_r, the energy deposition profile over depth x is given by:-

$$\frac{dE}{dx} = (E_p - E_r) f(\lambda) \exp(-f(\lambda)x)$$

where f(λ) is the silicon absorptivity at wavelength λ. For sensitive depth D and sensitive thickness Δ, the energy deposited in the sensitive volume is given by:-

$$\int_D^{D+\Delta} \frac{dE}{dx} dx = (E_p - E_r) \exp(-f(\lambda)D)(1 - \exp(-f(\lambda)\Delta))$$

Where:-

$$\int_0^\infty \frac{dE}{dx} dx = \frac{1}{f(\lambda)} \left. \frac{dE}{dx} \right|_{max} = E_p - E_r$$

The energies (E, E') deposited in the sensitive volume at the upset threshold at two (or more) wavelengths (λ, λ') may be equated to form expressions in D and Δ, for example:-

$$E \exp(-f(\lambda)D)(1 - \exp(-f(\lambda)\Delta)) = E' \exp(-f(\lambda')D)(1 - \exp(-f(\lambda')\Delta))$$

To find unique values of both D and Δ two such expressions are required, which necessitates measurements at three wavelengths.

However, even thresholds obtained for a single pair of wavelengths define a relationship between the sensitive layer depth D and the sensitive thickness Δ. This relationship is plotted for several ratios (5, 15 & 50) of the upset threshold pulse energy in infra red (1064nm) to that in green (532nm) in Figure 3. Note that a ratio of 50 would imply that D<2.3µm and Δ<10µm.

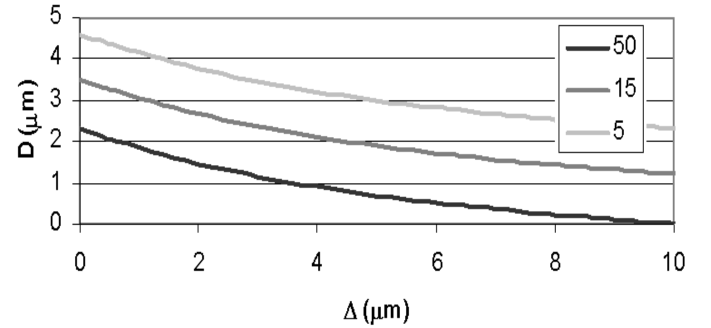

Figure 3: Sensitive layer depth D versus sensitive layer thickness Δ at three upset threshold ratios (1064nm:532nm).

It should be mentioned here that there are constraints on the accuracy of these laser measurements due to reflection, diffraction and interference effects associated particularly with the metallisation. These constraints will be considered further in Section V.

III. Generalisation of the Technique

The sensitive volume concept that a rectangular region of uniform sensitivity may be associated with each cell of the device is, of course, a gross simplification. In reality the cells are somewhat diffuse regions of continuously varying sensitivity and it is quite possible that there may exist two or more peaks of sensitivity within these regions, superimposed on the diffuse background. For example, auxiliary transistors are sometimes implemented in polysilicon layers above the main body of the silicon (as is the case for some of our test samples) and these might potentially give rise to subsidiary sensitivity peaks. However, it can be shown that the laser technique actually incorporates the potential explicitly to measure the precise depthwise variation in the sensitivity of cells.

If the sensitivity (more explicitly, the charge gathering efficiency) is defined as an unknown function sens(x) of the depth x beneath the silicon surface of the device, then the critical charge deposition Q_{crit} for upset to occur may be expressed as an integration over the product of sens(x) with the upset threshold laser pulse energy deposition rate at depth x (Figure 4). This laser energy deposition rate dE/dx is proportional to the absorbed laser pulse energy at the upset threshold E_{abs}, which may be expressed as a function of the silicon absorptivity $E_{abs}(f(\lambda))$, since it will be different for each test wavelength. We may write:-

$$\frac{dE}{dx} = E_{abs}(f(\lambda)) f(\lambda) \exp(-f(\lambda)x)$$

Hence,

$$Q_{crit} = \int_0^\infty E_{abs}(f(\lambda)) f(\lambda) sens(x) \exp(-f(\lambda)x) dx$$

On rearranging:-

$$\frac{Q_{crit}}{E_{abs}(f(\lambda))f(\lambda)} = \int_0^\infty sens(x)\exp(-f(\lambda)x)dx$$

It is usually a reasonable assumption (in fact an approximation) that the critical charge for upset is constant at all wavelengths for a particular device and the absorptivity is a well-established function of wavelength [6], [7]. Thus the left-hand side of the equation may be calculated empirically simply by measuring the absorbed laser pulse energy at the upset threshold for a wide range of wavelengths (i.e. for a wide range of absorptivities). Now the right-hand side of the equation is just the Laplace transform of the depthwise sensitivity profile in the absorptivity, hence sens(x) may in principle be derived by performing an inverse Laplace transform on the left-hand side result. It is also clear that the left-hand side should normally become proportional to 1/f(λ) as f(λ) tends to infinity (since the silicon should have some finite level of sensitivity at its front surface, so the threshold energy should become constant for large f(λ)). Furthermore, the left-hand side should be positive and decreasing for all values of f(λ)≥0. This follows from the observation that the value of the right-hand side must uniformly increase as f(λ) reduces.

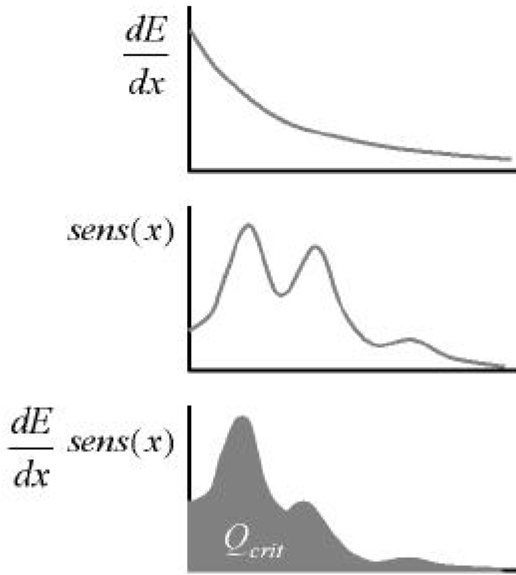

Figure 4: Critical charge as the integral of the product of the threshold pulse energy deposition with the sensitivity profile.

It should finally be noted that the reciprocal of the absorptivity 1/f(λ) provides a scale length for the distance over which the laser light is absorbed in the silicon. To obtain good results from this technique it will be necessary to test devices using laser pulses over a wavelength range such that 1/f(λ) varies from being smaller than the size of the smallest sensitivity features that are to be resolved to being larger than the overall size of the sensitive region.

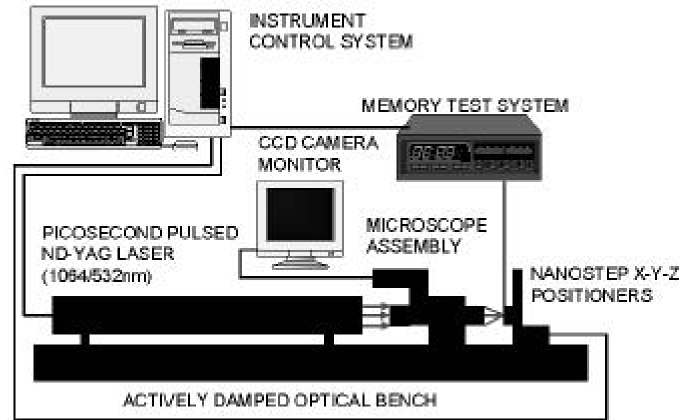

Figure 5: Diagram of the Single Event Radiation Effects in Electronics Laser (SEREEL) facility.

IV. Measurements

Laser pulse measurements of the upset cross-sections of a range of types of 1 Mbit SRAM device have been performed at both 1064nm and 532nm using the Matra BAe Dynamics Single Event Radiation Effects in Electronics Laser (SEREEL) facility (Figure 5). Each laser upset cross-section point was derived by delivering a large array of laser pulses (~1000 pulses when large numbers of errors were seen, increasing to ~6000 when only a few errors were observed) of fixed energy across the entire microchip die. The basic cross-section is the fraction of these laser pulses which produced a memory upset multiplied by the area of the chip (and divided by the number of bits on the device to scale from a chip cross-section to a bit cross-section). As examples, results for the Cypress CY7C109 (0.65µm feature size) and the Samsung KM681000A are shown in Figures 6 to 9. The devices were also tested at the CYCLONE ion beam facility at Louvain la Neuve, so these Figures give the laser data fitted to the ion beam cross-sections. (It should be noted that the ion beam data will only be used in an auxiliary argument in this paper: it is not required and has not been used for the main sensitive depth calculations.) Green and infrared cross-sections have also been obtained for the Mitsubishi M5M51008CFP and the Samsung KM681000B. The ratios of the threshold pulse energies at the two wavelengths for all these devices are given in Table 1. (Note that no ion data has been used in calculating these ratios: the laser pulse energies are measured directly during the laser testing). It may be observed that E_{ir} / E_{green} is generally not too different from 15 for the upset thresholds of these devices, which corresponds to the central curve in Figure 3.

It is necessary to take account of laser pulse energy reflected at the surface and at material interfaces in the device. Theoretically, the reflectivity of an interface has a predictable dependence on laser wavelength and incidence angle. However, the details of the real set of interfaces in a microchip are typically rather complicated. It is therefore considered more tractable and more reliable to seek to measure the actual reflected pulse energy in the experiment. This is feasible, because the CCD camera actually images the laser spot on the

chip surface. The brightness of this spot may be compared with the brightness of the laser spot when focussed on a highly reflective surface, such as a metallisation track (Figure 10). These observations suggest that absorbed pulse energy was about 50% of the incident pulse energy in both green and infrared for these experiments (with about a 10% standard error). However, work is ongoing to improve the accuracy of these measurements. (It should be noted that it is the incident pulse energy, which has been plotted in the Figures presented here.)

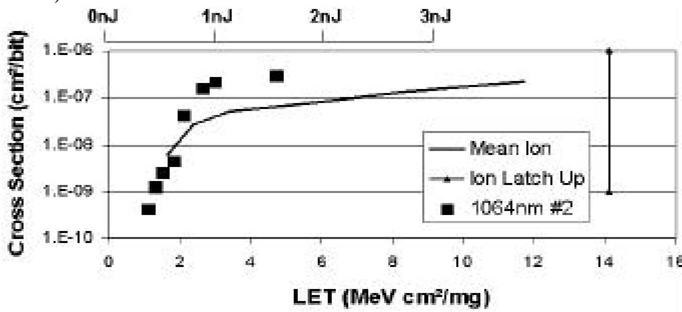

Figure 6: 1064nm Laser and Ion Beam Cross Sections For The Cypress CY7C109 (0.65μm) with 1nJ=3MeV/(mg/cm^2).

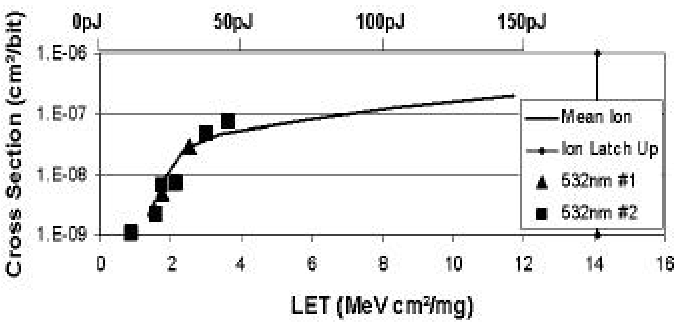

Figure 7: 532nm Laser and Ion Beam Cross Sections For The Cypress CY7C109 (0.65μm) with 12.5pJ=1MeV/(mg/cm^2).

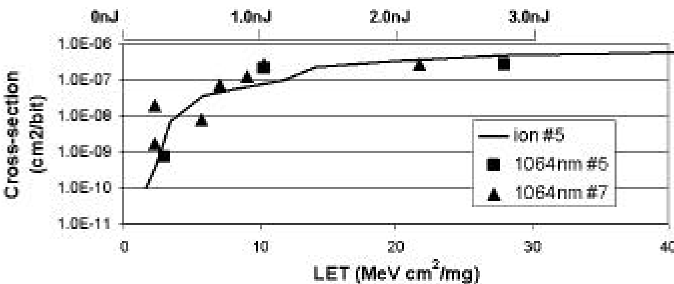

Figure 8: 1064nm Laser & Ion Cross-Sections for the Samsung KM681000A with 1nJ=10MeV/(mg/cm^2).

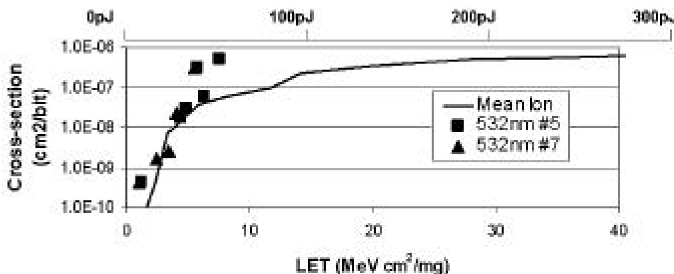

Figure 9: 532nm Laser & Ion Cross-Sections for the Samsung KM681000A with 6.67pJ=1MeV/(mg/cm^2).

The calibration factors, relating laser pulse energy to an equivalent LET, are plotted against feature sizes for eight 1Mbit SRAM types (those already mentioned above plus the Mitsubishi M5M51008A and M5M51008B, the Samsung KM681000E and the 0.42μm feature size version of the Cypress CY7C109) in Figure 11. By "calibration factor" is meant the ratio of the laser pulse energy threshold for upset to the LET threshold for upset in ion testing. It is so named because it is sometimes used to calibrate laser testing against ion testing. It is notable that there is a relatively flat trend (i.e. little dependence on feature size) with an average calibration factor just below 10pJ/(MeV/(mg/cm^2)).

Part No	Manufacturer & Feature Size	Threshold energy ratio 1064:532nm	Well depth (μm)
CY7C109	Cypress 0.65μm	26.67	5.4
M5M51008C	Mitsubishi 0.4μm	20.83	1.8
KM681000A	Samsung 0.7μm	14.99	6
KM681000B	Samsung 0.6μm	9.62	3.8

Table 1. Upset threshold infrared:green pulse energy ratios.

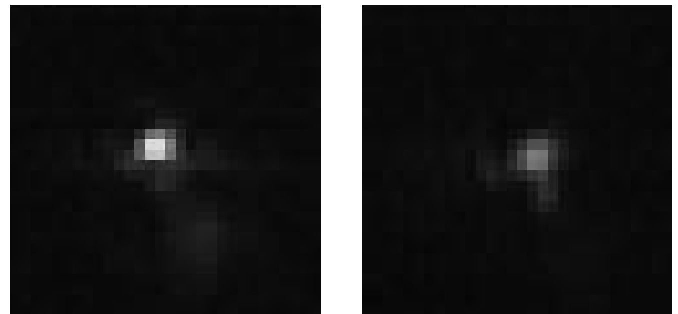

Figure 10: Laser spots at 532nm on metallisation (left) and silicon (right); the silicon reflectance is 54% of that from the metallisation and the pixel size is 0.45μm.

In parallel with the laser and ion beam testing, NMRC has performed detailed constructional analyses on samples of the same devices (from the same batches) [8]. The cross-sectional view of the M5M51008CFP shown in Figure 12 is an example of this work. The component is fabricated using a 0.35μm p-well process utilising two levels of metallisation and four levels of polysilicon on a non-epitaxial substrate, producing TFT-load SRAM cells. It was established that the n-channel transistor diffusion depth was 0.1μm and the well was 1.8μm deep. This sensitive region lies immediately beneath the gaps in polysilicon layer number 1 in Figure 7. However, in this design the cell loads are composed of p-channel thin film transistors formed from the overlying poly 3 and poly 4 layers. Furthermore, funnelling and diffusion may enable charge to be gathered even from the substrate beneath the well and the materials in which the polysilicon layers are embedded are observed to be optically transparent. Consequently, the real

picture is one of a varying profile of sensitivity over a depth range of at least ~5µm, possibly with two (or more) peaks for the different transistor elements in the cell. Clearly, there is no basis for any precise correspondence between observable features and the boundaries of the effective sensitive volume.

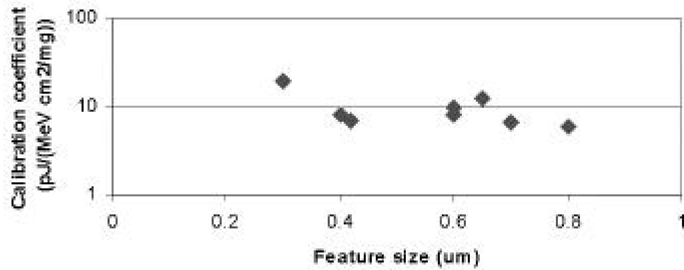

Figure 11: Green (532nm) calibration factors versus feature size.

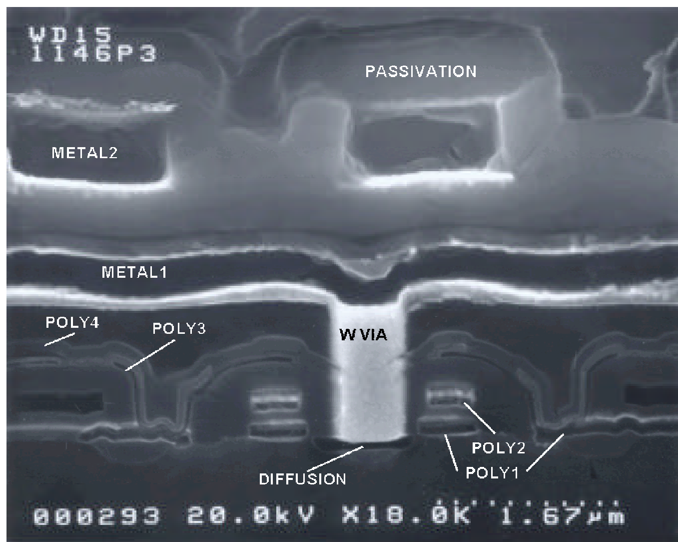

Figure 12: Cross-sectional view of the M5M51008CFP (x18000: the dotted scale is 1.67µm).

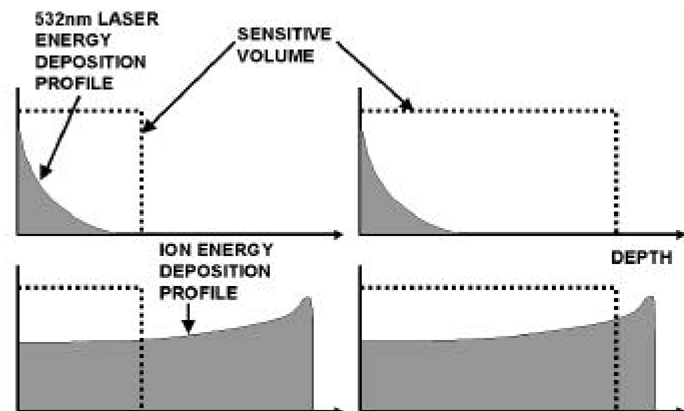

Figure 13: Trends in the sensitive volume energy deposition by 532nm laser pulses and by ions when the sensitive thickness changes.

V. DISCUSSION

The fact that the trend in the calibration factors at 532nm with feature size appears to be virtually flat is ostensibly surprising. It implies that the sensitive thickness of the memory cells is not scaling down with feature size for SRAM's in this feature size range (although it also possible that something else is scaling with feature size, so as to cancel out the expected trend). This is because the energy deposition by a green laser pulse should be expected to be static with decreasing feature size, because the penetration of this wavelength should remain small compared with the sensitive thickness. Conversely the charge collection from an ion of fixed LET should decline in proportion to any reduction in the sensitive thickness. The way in which the energy depositions for green laser pulses and for ions would be expected to change as the sensitive volume thickness changes is illustrated in the conceptual diagram of Figure 13. Consequently, the calibration factor of laser pulse energy at 532nm to equivalent LET should be approximately linearly proportional to feature size, if the sensitive thickness were scaling with feature size.

The NMRC analyses suggest that the silicon for all the present samples should contribute significantly to charge collection from ions and laser pulses from its front surface. This corresponds to a small effective sensitive depth D for the these experiments. However, the assumption of a small sensitive depth (e.g. D<1µm), together with the observation of infrared:green calibration factor ratios near 15, leads (see Figure 3) to a relatively large sensitive thickness Δ of 10 µm or more. However, this argument does not lead to a very precise value for the sensitive thickness: we would estimate a 90% confidence that the true values lie in the range 7µm to 25µm. This indicates significant charge collection from the substrate region in all our examples and a predominance of collection from the substrate for the smaller feature size devices. That there is significant charge collection from the substrate is indicated particularly by the well depth values in Table 1, which are taken from the NMRC sectional analyses and which show that the well depths are generally smaller than the sensitive thicknesses implied by the laser threshold ratios.

Both the invariance in the sensitive thickness in the trend of the green calibration factors and the indication of large effective sensitive thicknesses from the laser threshold ratios are in themselves tentative given the variations between individual data points and the limited set of examples. Nevertheless, these two types of observation are both consistent with an important role for charge deposited in the substrate. The most straightforward explanation is that the funnel effect is operating and charge generated in the substrate is readily flowing back up the conducting ionisation track to be collected onto the device node. It is worth noting that Melinger et al [6] also observed a less pronounced version of this effect for the 93L422 SRAM. These experimental results make the assumption of a 2 µm sensitive thickness, which is often adopted in the absence of better information (e.g. [2]), appear dubious.

In the ion beam approach to the measurement of the sensitive volume thickness, there is a risk of ions of the chosen species still causing upsets at near saturation levels after the Bragg peak has penetrated beyond the sensitive region. This would make it very difficult to get an accurate thickness as well as a depth for the sensitive region. Essentially it is necessary to choose an ion species with an LET in the Bragg peak which is just fractionally above the upset threshold for the device in order to obtain accurate results. This problem does not arise with laser pulses, because the pulse energy is trivially, continuously and precisely variable, such that pulse energy at the threshold may be measured at each experimental wavelength. Furthermore, the silicon absorptivity is such a strong function of wavelength that there is no real difficulty in varying the penetration of the laser pulses over the requisite range.

A further potential advantage of the laser technique is that it excludes metallisation layers and passivation oxide from the depth measurement. The laser spot is focussed on the silicon surface and will only penetrate where there is silicon. Ions may experience more variation in the effective depth of the sensitive volume across the chip surface due to the variable mass thickness of the superficial layers, which could lead to additional experimental error. In general, the increased flexibility and precision of the laser technique combined with the lower capital cost of the laser equipment would be expected to make it preferable to the ion beam methodology in most circumstances.

It should of course also be mentioned that the usual laser problem of metallisation potentially shadowing some sensitive areas or reducing the energy reaching sensitive regions continues to apply. Interference effects can also be set up by the diffraction of laser light among metallisation strips. However, the degree to which increasing numbers of metallisation layers will exclude laser light from entering via the front surface of devices is frequently overstated. It should be borne in mind that the light itself diffracts around small-scale obstacles and the charge it generates will rapidly diffuse behind them. Furthermore, these diffraction and diffusion processes tend to become more effective as the feature size decreases. In principle, the absorbed pulse energy can continue to be measured as the difference between the incident and reflected energies, even when the metallisation matrix leads to a large net reflectance. The problem is one of maintaining the accuracy of the measurement of the absorbed pulse energy in this circumstance. Some account may also need to be taken of the influence of doping concentrations on silicon absorptivity at the longer infrared wavelengths, but this is not a problem at visible wavelengths [7], [9].

It is clear from the analysis given in Section III that it is highly desirable to extend the number of wavelengths at which the laser measurements are performed. The Radiation Effects Group of Matra BAe Dynamics is therefore in the process of commissioning a Raman tube unit for the SEREEL system, which will make picosecond laser pulses available at several additional wavelengths in the most interesting range from 600nm to 700nm (orange-red).

VI. Conclusions

A laser method has been described and demonstrated, which measures the crucial sensitive volume parameters, that permit LET cross-section curves to be used to predict upset rates from proton and neutron fluxes. Since previous work [1] has shown that the laser system can also be used to generate the LET cross-section curves, it potentially constitutes a self-contained apparatus for making fast and economical proton, neutron and ion SEE predictions for large numbers of device types. It offers the prospect of an excellent high volume and low cost screening system. However, regular calibration of a laser system against real radiation sources is required to maintain confidence and accuracy.

It has also been shown that the laser technique is capable of being extended to measure the actual variations in the depthwise sensitivity profiles of microelectronic devices. This means that any problems with the technique due to the crudity of the sensitive volume approximation are addressable through a mere extension of the technique.

Finally, there are indications from two independent aspects of the laser tests conducted on a range of 1Mbit SRAM's at 1064nm and 532nm, that the sensitive thickness (or charge collection depth) of devices may not be scaling down with feature size. This appears to be due to a prominent role for charge gathered onto the sensitive nodes from the substrate, probably via the funnel effect (or possibly some other charge diffusion mechanism).

References

[1] Comparison Between SRAM Cross-Sections From Ion Beam Testing With Those Obtained Using A New Picosecond Pulsed Laser facility, R Jones, AM Chugg, CMS Jones, PH Duncan, CS Dyer & C Sanderson, IEEE Trans. Nuc. Sci., Vol. 47, No. 3, June 2000.

[2] A New Approach for the Prediction of the Neutron-Induced SEU Rate, C Vial, JM Palau, J Gasiot, MC Calvet and S Fourtine, IEEE Trans. Nucl. Sci., Vol. 45, 2915-20, December 1998.

[3] Microdosimetry Code Simulation of Charge-Deposition Spectra, Single Event Upsets and Multiple-Bit Upsets, CS Dyer, C Comber, PR Truscott, C Sanderson, C Underwood, M Oldfield, A Campbell, S Buchner and T Meehan, IEEE Trans. Nuc. Sci., Vol 46, 1486-93, December 1999.

[4] Threshold LET for SEU Induced by Low Energy Ions, PJ Mc Nulty, Ph Roche, JM Palau & J Gasiot, IEEE Trans. Nuc. Sci., Vol 46, 1370-77, December 1999.

[5] Using A Carbon Beam As A Probe To Extract The Thickness Of Sensitive Volumes, C Inguimbert et al, IEEE Trans. Nuc. Sci., Vol. 47, No. 3, June 2000.

[6] Pulsed Laser-Induced Single Event Upset and Charge Collection Measurements as a Function of Optical Penetration Depth, JS Melinger, D McMorrow, AB Campbell, S Buchner, LH Tran, AR Knudson and WR Curtice, Journal of Applied Physics, Vol. 84, No. 2, July 1998.

[7] Charge Generation and Collection in p-n Junctions Excited with Pulsed Infrared Lasers, AH Johnston, IEEE Trans. Nuc. Sci., Vol 40, 1694-1702, December 1993.

[8] Constructional Analysis Report Number DTE1146, R Allison, T O'Shea, R Fitzgerald, NMRC, February 2001.

[9] Critical Evaluation of the Pulsed Laser Method for Single Event Effects Testing and Fundamental Studies, JS Melinger, S Buchner, D McMorrow, WJ Stapor, TR Weatherford and AB Campbell, IEEE Trans. Nucl. Sci., Vol. 41, 2574-84, December 1994.